

# Low-loss saturable absorbers based on tapered fibers embedded in carbon nanotube/polymer composites

Amos Martinez, Mohammed Al Araimi, Artemiy Dmitriev, Petro Lutsyk, Shen Li, Chengbo Mou, Alexey Rozhin, Misha Sumetsky, and Sergei Turitsyn

Citation: *APL Photonics* **2**, 126103 (2017);

View online: <https://doi.org/10.1063/1.4996918>

View Table of Contents: <http://aip.scitation.org/toc/app/2/12>

Published by the American Institute of Physics

---

## Articles you may be interested in

Dielectric broadband meta-vector-polarizers based on nematic liquid crystal

*APL Photonics* **2**, 126102 (2017); 10.1063/1.5006016

Single-photon detectors combining high efficiency, high detection rates, and ultra-high timing resolution

*APL Photonics* **2**, 111301 (2017); 10.1063/1.5000001

Robust nano-fabrication of an integrated platform for spin control in a tunable microcavity

*APL Photonics* **2**, 126101 (2017); 10.1063/1.5001144

Fiber chirped pulse amplification of a short wavelength mode-locked thulium-doped fiber laser

*APL Photonics* **2**, 121302 (2017); 10.1063/1.4996441

Multi-planar amorphous silicon photonics with compact interplanar couplers, cross talk mitigation, and low crossing loss

*APL Photonics* **2**, 116101 (2017); 10.1063/1.5000384

Nanodiamonds with photostable, sub-gigahertz linewidth quantum emitters

*APL Photonics* **2**, 116103 (2017); 10.1063/1.4998199

---



# Low-loss saturable absorbers based on tapered fibers embedded in carbon nanotube/polymer composites

Amos Martinez,<sup>1,a,b</sup> Mohammed Al Araimi,<sup>1,2</sup> Artemiy Dmitriev,<sup>1,c</sup>  
 Petro Lutsyk,<sup>1</sup> Shen Li,<sup>1</sup> Chengbo Mou,<sup>3</sup> Alexey Rozhin,<sup>1</sup> Misha Sumetsky,<sup>1</sup>  
 and Sergei Turitsyn<sup>1</sup>

<sup>1</sup>Aston Institute of Photonic Technologies, Aston University, Birmingham B4 7ET, United Kingdom

<sup>2</sup>Engineering Department, Al Musanna College of Technology, Muladdah Musanna, P.O. Box 191, P.C. 314, Sultanate of Oman

<sup>3</sup>Key laboratory of Specialty Fiber Optics and Optical Access Networks, Joint International Research Laboratory of Specialty Fiber Optics and Advanced Communication, Shanghai Institute for Advanced Communication and Data Science, Shanghai University, Shanghai 200444, P.R. China

(Received 19 July 2017; accepted 26 November 2017; published online 14 December 2017)

The emergence of low-dimensional materials has opened new opportunities in the fabrication of compact nonlinear photonic devices. Single-walled carbon nanotubes were among the first of those materials to attract the attention of the photonics community owing to their high third order susceptibility, broadband operation, and ultrafast response. Saturable absorption, in particular, has become a widespread application for nanotubes in the mode-locking of a fiber laser where they are used as nonlinear passive amplitude modulators to initiate pulsed operation. Numerous approaches have been proposed for the integration of nanotubes in fiber systems; these can be divided into those that rely on direct interaction (where the nanotubes are sandwiched between fiber connectors) and those that rely on lateral interaction with the evanescence field of the propagating wave. Tapered fibers, in particular, offer excellent flexibility to adjust the nonlinearity of nanotube-based devices but suffer from high losses (typically exceeding 50%) and poor saturable to non-saturable absorption ratios (typically above 1:5). In this paper, we propose a method to fabricate carbon nanotube saturable absorbers with controllable saturation power, low-losses (as low as 15%), and large saturable to non-saturable loss ratios approaching 1:1. This is achieved by optimizing the procedure of embedding tapered fibers in low-refractive index polymers. In addition, this study sheds light in the operation of these devices, highlighting a trade-off between losses and saturation power and providing guidelines for the design of saturable absorbers according to their application. © 2017 Author(s). All article content, except where otherwise noted, is licensed under a Creative Commons Attribution (CC BY) license (<http://creativecommons.org/licenses/by/4.0/>). <https://doi.org/10.1063/1.4996918>

## INTRODUCTION

Passive mode-locking is the preferred technique for the generation of ultrashort pulses in fiber lasers. This technique consists in introducing a device or material, a saturable absorber, which absorbs the incident light nonlinearly.<sup>1</sup> The saturable absorber operates as a passive self-amplitude optical modulator that increases its optical transmission with high peak powers.<sup>2,3</sup> Mode-locked pulsed operation originates when noise fluctuations of higher intensities in the laser cavity begin to saturate the absorber, reducing its losses. This noise spike is further amplified by the gain media in subsequent

<sup>a</sup>Author to whom correspondence should be addressed: [a.martinez3@aston.ac.uk](mailto:a.martinez3@aston.ac.uk).

<sup>b</sup>Currently at Toshiba Research Europe Ltd., Cambridge CB40GZ, United Kingdom.

<sup>c</sup>Currently at School of Physics and Astronomy, University of Birmingham, Birmingham B15 2TT, United Kingdom.

round trips, increasing its intensity and further saturating the losses until a train of pulses stabilizes. The main parameters to consider in saturable absorbers are operating wavelength range, saturation fluence, non-saturable loss, modulation depth, and recovery time. Carbon nanotube (CNT) saturable absorbers were first proposed over a decade ago.<sup>4</sup> That first demonstration highlighted the broadband operation and fast recovery time of carbon nanotube saturable absorbers. In addition, unlike most commercial saturable absorbers at that time, carbon nanotube films could be easily integrated into optical fibers by spray-coating,<sup>4</sup> optical deposition,<sup>5</sup> or sandwiching a CNT-polymer thin film between two fiber connectors.<sup>6</sup> Successful demonstrations with CNTs were followed by the demonstration of saturable absorption in graphene<sup>7,8</sup> opening up a race to find other two-dimensional (2D) layered materials that could operate as saturable absorbers including several transition metal dichalcogenides,<sup>9</sup> topological insulators,<sup>10</sup> or black phosphorous.<sup>11,12</sup>

The simplicity of integration of the carbon nanotubes and 2D-layered materials in photonic devices has allowed for the design of more complex schemes aiming to maximize the performance of the device by exploiting interaction between the nanomaterial and the evanescent field of the propagating wave. In these schemes, CNTs interact with the tail of the propagating wave that leaks out of waveguide structures such as tapered-fibers,<sup>5,13</sup> D-shaped fibers,<sup>14</sup> fiber microchannels,<sup>15</sup> or hollow-core optical fibers<sup>16</sup> into the surrounding media. These schemes were first proposed to overcome (or mitigate) the optical power-induced damage, but they are also an efficient approach to enhance the nonlinearity of the device by extending the lateral interaction length.

Among evanescent field interaction schemes, CNT-coated tapered-fiber saturable absorbers appear to be the most versatile. The fabrication of CNT-fiber microchannels<sup>15</sup> requires complex and expensive equipment, and it is time-consuming. The use of CNT-filled hollow-core fibers<sup>16</sup> relies on specialty fibers with fixed parameters, and while CNT-coated D-shaped fibers have been shown to be efficient saturable absorbers,<sup>14</sup> they have a strong polarization dependence, undesired for some laser systems. On the other hand, CNT-coated tapered fibers are polarization insensitive and, by controlling the taper's waist and length, we can control the interaction length and the percentage of power and power density that leaks into the evanescent field.

CNT-based tapered fiber devices have been previously fabricated by directly spray-coating<sup>13</sup> or optical depositing<sup>5</sup> the CNTs in bare tapered fibers. However, by depositing the CNTs directly in the taper's surface, these devices suffer from extremely large scattering losses limiting the length of interaction unless multimode tapered fibers with large waist diameters in the order of 10s microns are used. In addition, these tapered fibers are directly exposed to the environment and deteriorate rapidly making them unsuitable for most practical applications.

An alternative solution consists in coating the tapered fiber with a low refractive index CNT-polymer composite.<sup>17</sup> The main advantages of this approach over spray-coating and optical deposition are threefold: (1) the polymer composite protects the tapered fiber from the environment ensuring long term reliability, (2) CNTs can be efficiently dispersed in the polymer matrix minimizing bundling and agglomeration of the nanotubes, reducing device losses, and allowing for the fabrication of devices with longer interaction lengths and thinner waist diameters, (3) since the CNTs are not in direct contact to the surface of the tapered fiber, scattering losses can be significantly reduced. Besides saturable absorption, tapered fibers coated with CNT-polymer devices have been used for four-wave mixing based wavelength conversion,<sup>18</sup> where the long lateral interaction length of the tapered fiber is used to enhance the third order nonlinearity of the device.

Although tapered fibers coated with a low refractive index CNT-polymer composite offer excellent flexibility to adjust the dimensions and nonlinearity of nanotube-based fiber devices, they still suffer from relatively high losses (typically exceeding 50%) and a modest saturable to non-saturable loss ratio (e.g., approximately 1:8 in Ref. 18).

In this paper, we demonstrate the fabrication of CNT saturable absorbers with low losses and high saturable to non-saturable loss ratios. We achieve this by careful optimization of the fabrication parameters, including (1) the mixing and concentration of CNTs in the polymer matrix to minimize excessive scattering losses, (2) the dimensions and fabrication of the tapered fibers, and (3) the final deposition and thermal treatment of the CNT-polymer mixture in the tapered fiber. In addition, we show how the saturation power, a key parameter in determining the power required to self-start passive mode-locked operation, can be efficiently controlled by adjusting the taper's waist diameter.

For instance, we show a CNT-coated taper saturable absorber with linear losses of 25%, a saturable to non-saturable ratio of 1:3, and a saturation power of 0.45 mW using a taper with a waist diameter as thin as 3  $\mu\text{m}$ . While we also demonstrate devices with lower losses and higher saturable to non-saturable ratios, this comes at the expense of using tapers with larger waist diameters, leading to a significant increase in the saturation power (e.g., 5 mW for a 5.3  $\mu\text{m}$  waist diameter). Thus, this study highlights a trade-off between non-saturable losses and saturation power providing guidelines for the design of saturable absorbers according to the requirements of each specific application either as a saturable absorber for fiber laser applications or four-wave mixing.

### Device fabrication

In this section, we describe the fabrication of CNT-polymer embedded tapered fibers. First, low-refractive index CNT-polymer composites are prepared. Following the approach proposed by Xu *et al.*,<sup>18</sup> we use a commercially available low refractive index polymer ( $n = 1.42$ ) poly 2,2,2-trifluoroethyl methacrylate (PTFEMA) and commercially available single-walled carbon nanotubes fabricated by the high pressure CO (HiPCO) process. 2 mg of HiPCO CNTs are placed in 20 ml of N-methyl-2-pyrrolidone (NMP). Unlike<sup>17</sup> where di-methyl-formamide (DMF) is used as a solvent; here we use NMP, as it is well known for its efficiency in the direct dispersion of CNTs at concentrations below 0.02 mg ml<sup>-1</sup> (Ref. 6). The mixture is then subjected to sonication using a commercial ultrasonic processor for 1 h at 200 W and 20 kHz. The dispersion is immediately ultracentrifuged for 2 h 30 min at 17 °C using (MLS 50 rotor) at 45 k revolutions per minute (RPM) to remove impurities and residual bundles. The normalized optical transmission and photoluminescence excitation-emission (PLE) map of HiPCO CNTs mixed in NMP after sonication and centrifugation are shown in Figs. 1(a) and 1(b), respectively.

Single-walled CNTs are formed when a single-layer graphene is rolled seamlessly to form a quasi-one-dimensional (1D) cylinder. This adds an additional level of electron confinement in graphene's electronic density of states (e DOSs) leading to CNTs having a quantized e DOS with distinct Van Hove singularities characteristic of 1D structures. Whether a CNT is metallic or semiconducting is determined by the orientation of the carbon lattice with respect to the axis of the nanotube with one third of the CNTs behaving as metals and two thirds as direct bandgap semiconductors.<sup>19</sup>

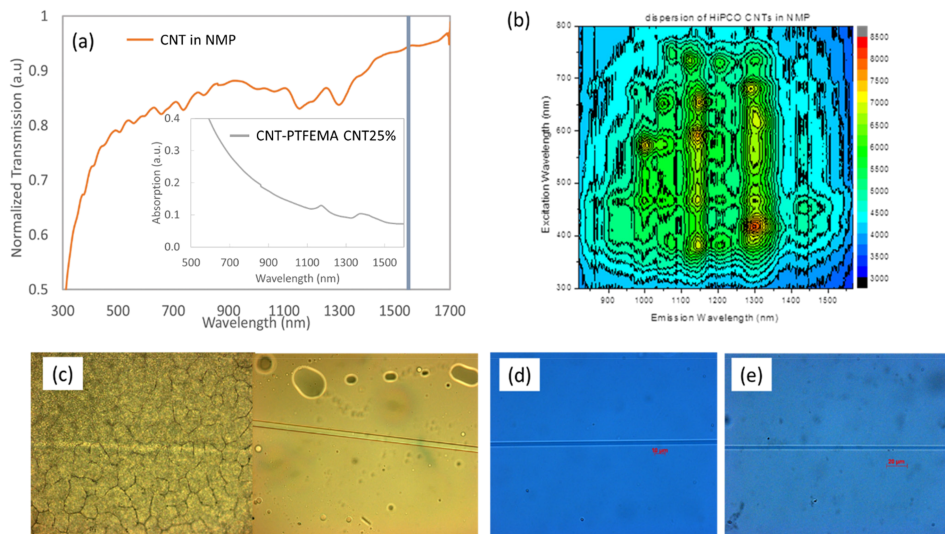


FIG. 1. (a) Linear optical transmission of dispersion of HiPCO CNTs in NMP (gray vertical line marks the 1550 nm wavelength). (inset) Absorption of CNT-PTFEMA thin film with 25% CNT concentration (b) Photo-luminescence excitation-emission (PLE) map of the HiPCO CNTs in NMP. (c) Microscope images of a CNT-coated taper fiber before (left) and after (right) thermal treatment. (d) Microscope image of a 4.0  $\mu\text{m}$  taper fiber coated with a CNT-PTFEMA polymer composite with 75% concentration. (e) Microscope image of a 3.0  $\mu\text{m}$  taper fiber coated with a CNT-PTFEMA polymer composite with 100% concentration.

TABLE I. Ratio of CNT-NMP to neat NMP in the preparation of CNT-PTFEMA composites. The CNT-NMP dispersion is made by mixing 2 mg of CNT per 20 ml of NMP.

Sample	Initial CNT-NMP dispersion in ml per g of PTFEMA	Neat NMP in ml
100% CNTs	1	0
75% CNTs	0.75	0.25
50% CNTs	0.5	0.5
25% CNTs	0.25	0.75
0% CNTs	0	1

Semiconducting CNTs absorb incoming photons when the incident photon's energy is resonant with the energy bandgap of one of the allowed CNT inter-band transitions (i.e., between Van Hove singularities symmetric with respect to the Fermi level) with optical absorption peaking at a wavelength resonant with the first semiconducting transition,  $E_{11}$  (i.e., between the first Van hove singularities in conduction and valence bands). Since  $E_{11}$  is inversely proportional to the diameter of the single-wall CNT, the central absorption wavelength is directly proportional to the nanotubes' diameter.

The HiPCO process produces CNTs with a large range of nanotube diameters leading to the broad absorption bands of these devices. Figures 1(a) and 1(b) confirm a broad resonant absorption of the  $E_{11}$  transition of the HiPCO CNTs centered at approximately 1300 nm and stretching into the  $\text{Er}^{3+}$  fiber laser emission window. Consequently, Figs. 1(a) and 1(b) also confirm that the majority of the CNTs in the device will not contribute to the resonant absorption at the fiber laser emission wavelength. Thus, an additional stage of separation and selection of CNTs by the tube diameter should, in principle, allow further improvements in the performance of these devices.

After centrifugation, the top 70% of the resultant dispersion is used as initial CNT dispersion and mixed with 1 g of PTFEMA to prepare CNT-NMP-PTFEMA mixtures with a range of CNT concentrations as summarized in Table I. To vary the concentration of CNTs, the volume of admixed initial CNTs dispersion is reduced and neat NMP is added to keep the total polymer concentration at 1 g/ml (samples of 75%-25% CNTs). A sample with 0% CNTs (consisting of PTFEMA only) is also studied as a reference.

Once the polymer mixtures are ready, we fabricate biconical tapered fibers with waist diameters of 5.3  $\mu\text{m}$ , 4.0  $\mu\text{m}$ , 3.0  $\mu\text{m}$ , and 2.2  $\mu\text{m}$  from regular single-mode optical fibers with an initial fiber diameter of 125  $\mu\text{m}$  by indirect  $\text{CO}_2$  laser heating and pulling technique.<sup>20</sup> The fiber is placed inside a sapphire tube with inner and outer diameters of, respectively, 0.9 mm and 1.6 mm that act as a micro-furnace. Unfocused continuous wave (CW) radiation of the  $\text{CO}_2$  laser (central wavelength at 10.6  $\mu\text{m}$ ) is incident on the sapphire tube, heating it to the temperature corresponding to silica softening. The optical fiber is drawn in cycles by gradual stretching while moving through the tube in both directions. Typical propagation losses of the free standing tapered fibers range from 4% to 7%. The final length of the tapers ranges from 25 mm to 31 mm (depending on the waist thickness) with a waist length of approximately 4 mm.

The tapered fibers are fixed to a glass plate and fully coated with the CNT-NMP-PTFEMA mixture. The coated tapered fibers are then immediately placed in an oven at 60 °C (slightly above the melting point for the PTFEMA at ca. 50 °C) until the NMP solvent fully evaporates (typically we leave it overnight). This thermal treatment is crucial toward ensuring the homogeneity and transparency of the final CNT-PTFEMA composite. Figures 1(c)–1(e) show microscopic photographs of CNT-PTFEMA coated tapered fibers. Figure 1(c) compares the transparency of the polymer without (left) and with (right) thermal treatment. Without thermal treatment, the polymer loses its transparency, appearing whitish to the naked eye and making it unsuitable for optical applications. Figures 1(d) and 1(e) show tapered fibers with waist diameters of 4.0  $\mu\text{m}$  and 3.0  $\mu\text{m}$  coated with CNT-PTFEMA composites with CNT concentrations of 75% and 100% (CNT concentration as defined in Table I).

### Nonlinear saturable absorption of CNT-coated tapered-fiber devices

Saturable absorption is a nonlinear process where the optical transmission of a material increases at high incident light intensities. Saturable absorption is related to the imaginary part of the 3rd order

nonlinearity,  $\text{Im } \chi^{(3)}$ . Its real part,  $\text{Re } \chi^{(3)}$ , responsible for the nonlinear refractive index ( $n_2$ ), has been recently reported to be as high as  $1.27 \times 10^{-14} \text{ m}^2 \text{ W}^{-1}$  ( $2.2 \times 10^{-8} \text{ esu}$ ) experimentally in single-walled carbon nanotubes, where the nanotube diameter distribution was carefully selected.<sup>21</sup> A high  $\text{Re } \chi^{(3)}$  is desirable in nonlinear photonic applications such as all-optical signal processing,<sup>22</sup> wavelength conversion,<sup>18</sup> and photon-pair generation.<sup>21</sup> Nonlinear devices where the nonlinearity of the device can be enhanced by extending the interaction length such as the CNT-polymer coated tapered fibers proposed here also hold great potential for  $\text{Re } \chi^{(3)}$  nonlinear photonic applications.

In this work, we are interested in studying the imaginary part of  $\chi^{(3)}$ , the saturable absorption, of tapered fibers embedded in CNT-PTFEMA composites. Saturable absorption is a key function in the passive mode-locking of lasers where the absorber is “bleached” at higher intensities, discriminating in favor of high intensity pulsed operation. When evaluating saturable absorbers, we must consider several parameters including the modulation depth ( $\alpha_o$ ), non-saturable losses ( $\alpha_{NS}$ ), and saturation power ( $P_{Sat}$ ). We use the setup depicted in Fig. 2(a) to measure power dependent losses ( $\alpha(P)$ ) for three tapered fibers with waist diameters of  $5.3 \mu\text{m}$ ,  $3.0 \mu\text{m}$ , and  $2.2 \mu\text{m}$  coated with CNT-PTFEMA composites with a 50% concentration (as defined in Table I). In addition, we study the saturable absorption of a reference sample where a tapered fiber with a waist diameter of  $5.3 \mu\text{m}$  is coated with PTFEMA (i.e., without CNTs). Our experimental data are fitted to the instantaneous saturable absorber model<sup>23</sup> [expressed in Eq. (1)] to extrapolate the approximate values of  $\alpha_o$ ,  $\alpha_{NS}$ , and  $P_{Sat}$ ,

$$\alpha(P) = \frac{\alpha_o}{1 + P/P_{Sat}} + \alpha_{NS}, \quad (1)$$

where  $P$  is the incident optical power,  $\alpha_o$  is the modulation depth,  $\alpha_{NS}$  are the nonsaturable absorption losses, and  $P_{Sat}$  is the saturation power.

We first look at the power dependent losses of a tapered fiber with a waist diameter of  $5.3 \mu\text{m}$  and coated with PTFEMA (i.e., without CNTs), shown in Fig. 2(b). We can see that absorption losses remain constant with increasing input powers, ruling out saturable absorption in the PTFEMA polymer itself. Insertion losses of this device were approximately 9%, compared to 4%–7% insertion losses in tapers suspended in air. Higher losses in PTFEMA coated tapered fibers are expected owing to the increased refractive index (1.42) leading to a higher fraction of the propagating wave power leaking into the evanescent field. Taking this into account, we can consider both the linear absorption and nonlinear absorption of PTFEMA negligible at 1550 nm.

Figures 2(c)–2(e) show the power dependent losses for 3 tapered fibers with waist diameters of  $5.3 \mu\text{m}$ ,  $3.0 \mu\text{m}$ , and  $2.2 \mu\text{m}$ , respectively, and coated with HiPCO CNTs with 50% concentration level (as defined in Table I). The laser used to carry out power dependent losses was a mode-locked fiber laser emitting 600 fs pulses with a 25 MHz repetition rate.

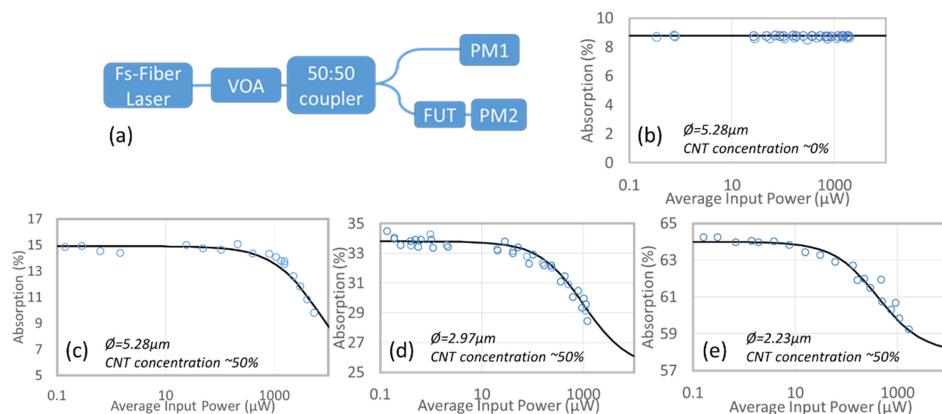


FIG. 2. (a) Setup used to measure power dependent losses of the devices. VOA—variable optical attenuator, FUT—fiber under test, PM—power-meter. (b) Losses of PTFEMA-coated taper fiber with a  $5.3 \mu\text{m}$  waist diameter (without CNTs). [(c)–(e)] Power dependent losses of CNT-PTFEMA coated taper fibers with 50% CNT concentration (as defined by Table I) and waist diameters of  $5.3 \mu\text{m}$  (c),  $3.0 \mu\text{m}$  (d), and  $2.2 \mu\text{m}$  (e).

TABLE II. Laser performance of the fiber laser operating at its mode-locked threshold when mode-locked by taper-fiber-based saturable absorbers with a fixed CNT concentration and varying taper waist diameter.

$\phi$ ( $\mu\text{m}$ )	CNT concentration (%)	$\alpha_0$ (%)	$P_{\text{Sat}}$ (mW)	$\alpha_{ns}$ (%)	$\Delta\lambda$ (nm)	$\tau_p$ (fs)	TBP
5.3	50	8	5	7	2.1	$\sim 1500$	0.38
3.0	50	8.5	0.45	25.3	5.7	$\sim 450$	0.31
2.2	50	6	0.41	58	7.8	$\sim 330$	0.31

The saturable absorption measurements reveal several interesting features of these saturable absorbers. First, the devices exhibit significantly lower insertion losses than those revealed by similar nanomaterial coated devices in the literature, with values of approximately 15% and 34% for tapers of waist diameters  $5.3 \mu\text{m}$  and  $3.0 \mu\text{m}$ , respectively. More importantly, the devices show impressive saturable to non-saturable ratios for such devices with the ratios of approximately 0.35 and 0.1 for the tapers with waist diameters  $3.0 \mu\text{m}$  and  $2.2 \mu\text{m}$ , respectively, compared to ratios in the literature typically lower than 0.1. Interestingly, the taper with  $5.3 \mu\text{m}$  waist diameter and 15% linear losses exhibited extremely high saturable to non-saturable ratio for this type of device at approximately 1.2 (Table II in the section titled Discussion details the nonlinear absorption parameters for these three saturable absorbers).

Aside from modulation depth and non-saturable losses, the saturable absorption measurements reveal an important feature in the saturation power of tapered fiber saturable absorbers. We observe a decrease in the saturation power of more than one order of magnitude as we decrease the taper waist diameter: from 5 mW (taper with waist diameters of  $5.3 \mu\text{m}$ ) to 0.45 mW ( $3.0 \mu\text{m}$ ) and 0.41 mW ( $2.2 \mu\text{m}$ ). This is not surprising since smaller waist diameters lead to lower saturation powers resulting from the higher power density at surface and a higher ratio of power in the evanescent field in thinner tapers.<sup>24</sup> However, it is a key factor to take into consideration when designing taper-based saturable absorbers as it highlights the importance of using tapers with small waist diameters (to decrease the saturation power and consequently the mode-locking threshold).

Summarizing, in the designing of saturable absorbers based on tapered fibers coated with CNTs, there is a trade-off between non-saturable losses and saturation power. Considering the high single-pass cavity gain in fiber lasers, where moderate losses can be tolerated, we find that waist diameters in a range from  $4 \mu\text{m}$  to  $2 \mu\text{m}$  and CNT concentration of 50% to 75% would suit most applications in the saturable absorption of fiber lasers since they combine moderate losses, good saturable to non-saturable ratios, and low saturation powers.

### Fiber laser passive modelocking by CNT-PTFEMA coated tapered-fibers

To test the performance of the CNT-PTFEMA coated tapered fiber devices as saturable absorbers, we incorporate them into an  $\text{Er}^{3+}$ -doped fiber laser, as depicted in Fig. 3. The laser is pumped by a 975 nm laser diode (LD), using a 980/1550 wavelength division multiplexer (WDM). The gain section of the laser consists of 1.1 m of erbium doped fiber (EDF) with 80 dB/m at 1530 nm nominal absorption and group velocity dispersion of +59 ps<sup>2</sup>/km. A single fiber isolator ensures unidirectional operation

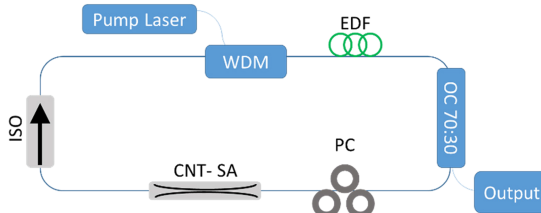


FIG. 3. Ring-cavity  $\text{Er}^{3+}$  doped fiber laser used to test the performance of the CNT-PTFEMA coated tapered fiber saturable absorbers as mode-locking devices. WDM—wavelength division multiplexer, EDF—erbium doped fiber, OC 70:30—output coupler delivering 70% of the light back in the laser cavity and 30% as output, PC—polarization controller, CNT-SA—carbon nanotube-based saturable absorber, ISO—isolator.

in the laser cavity and a standard 70:30 coupler provides 30% laser output, the remaining 70% being sent back into the cavity for feedback. The rest of the laser cavity includes 1.22 m of OFS980 fiber and approximately 5 m of standard single mode fiber, SMF 28 fiber, including the CNT-PTFEMA coated tapered fiber saturable absorber that is spliced into the cavity between a polarization controller (PC) and the isolator.

CW lasing starts at a pump power of 13 mW for the tapered fibers with waist diameters of  $5.3 \mu\text{m}$  and  $3 \mu\text{m}$  and 15 mW for the tapered fiber with  $2.2 \mu\text{m}$  waist. Mode-locked laser operation self-starts at pump powers of 14 mW for the  $5.3 \mu\text{m}$  and  $3 \mu\text{m}$  waist tapers and 16 mW for the  $2.2 \mu\text{m}$  waist taper fiber. At these powers, the laser operates in its fundamental continuous wave mode-locked operation for all three absorbers (i.e., emitting one single pulse per cavity round trip). Single-pulse laser operation remains stable regardless of the orientation of the polarization controller in the cavity.

Besides single-pulse operation, we observed various multi-pulsing regimes (when multiple pulses co-exist in the cavity at any one time) by increasing the pump power. Multi-pulsing regimes such as harmonic mode-locking, tight bound solitons, and soliton molecules formed by three and four pulses were observed at higher pump powers, but these regimes will not be discussed in this paper. However, it is worth mentioning that the transition from single to multi-pulsing takes place at higher powers for tapers with stronger saturation (those with smaller waist diameters and higher concentrations).

Figure 4 summarizes the performance of the laser with the three saturable absorbers at their mode-locking thresholds. Figures 4(a)–4(c) show the optical spectrum for the three devices and their respective autocorrelator traces (inset). Autocorrelator measurements required amplification of the pulses before the autocorrelator. We used a commercial erbium doped fiber amplifier (EDFA) that adds some additional nonlinearities and dispersion, resulting on some pulse distortion and the presence of a pedestal in the autocorrelator traces.

Optical spectra and autocorrelation traces from Fig. 4 are fitted to the squared hyperbolic secant ( $\text{sech}^2$ ) function (black dashed curves), characteristic of soliton propagation. The pulse-width ( $\tau_p$ ),

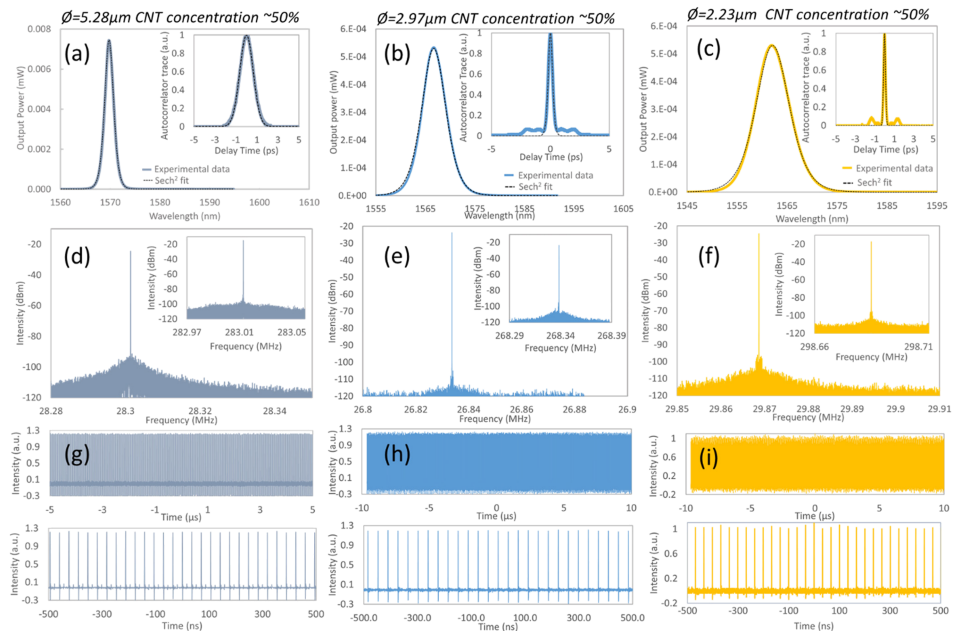


FIG. 4. Characterization of the performance of an  $\text{Er}^{3+}$  doped fiber laser mode-locked by taper fibers coated with CNT-PTFEMA composite with 50% CNT concentration (concentration % is defined in Table I). [(a)-(c)] Optical spectrum and autocorrelator trace (insets) of the fiber laser using CNT-PTFEMA coated tapers with waist diameters of  $5.3 \mu\text{m}$  (a),  $3.0 \mu\text{m}$ , (b) and  $2.2 \mu\text{m}$  (c). [(d)-(f)] RF Spectra of the fundamental and 10th harmonics (insets) with 3 Hz resolution and over a 100 kHz span for waist diameters of  $5.3 \mu\text{m}$  (d),  $3.0 \mu\text{m}$  (e), and  $2.2 \mu\text{m}$  (f). [(g)-(i)] Oscilloscope traces over  $10 \mu\text{s}$  (top) and  $1 \mu\text{s}$  (bottom) spans for tapers with waist diameters of  $5.3 \mu\text{m}$  (g),  $3.0 \mu\text{m}$  (h), and  $2.2 \mu\text{m}$  (i).

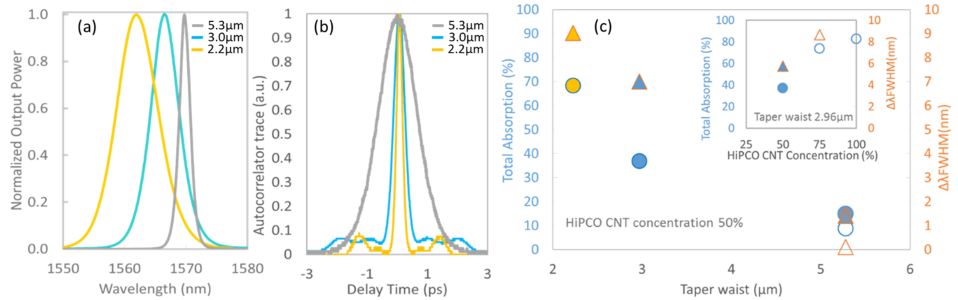


FIG. 5. Comparison of spectral bandwidth (a) and pulse duration (b) for the fiber lasers operating at their threshold pump powers (14 mW to 16 mW) with three taper-based saturable absorbers with 5.3  $\mu\text{m}$  (gray), 3.0  $\mu\text{m}$  (blue), and 2.2  $\mu\text{m}$  (yellow) waist diameters and coated with a CNT-PTFEMA composite with 50% concentration. Results show evidence of pulse shortening with decreasing waist diameters. (c) Comparison of total taper absorption (circles) and laser output spectral bandwidth (triangles) with a decreasing waist diameter and (inset) increasing CNT concentration at a pump power of 18 mW. Note that due to the large insertion losses, stable pulse operation was not achieved with the taper with a waist diameter of 3.0  $\mu\text{m}$  and 100% CNT concentration. Note also that the broader spectral bandwidths observed in (c) compared to (a) and (b) result from the slightly higher pump power used (18 mW). Color references yellow, blue, and gray in (c) correspond to devices shown in (a) and (b) of the same color.

spectral bandwidth ( $\Delta\lambda$ ), and time-bandwidth product (TBP) for the three samples are summarized in Table II. These results show that saturable absorbers made with thinner tapers generate pulses with broader spectral bandwidths and shorter pulse durations.

The RF signal of the laser output at its fundamental (and 10th order) frequency is shown in Figs. 4(d)–4(f) (insets). RF signals are measured with a resolution of 3 Hz and show signal to noise ratios (SNR) of >70 dB. Finally, the pulse trains were captured over time periods of 1  $\mu\text{s}$  and 20  $\mu\text{s}$  with a fast oscilloscope with 12 ps steps [Figs. 4(g)–4(i) show the pulse trains].

## Discussion

In Fig. 5, we compare the performance of CNT-PTFEMA coated taper fiber saturable absorbers with different waist diameters and different CNT concentrations. To evaluate the performance, we use three key markers: insertion losses, spectral bandwidth, and pulse duration. Figures 5(a)–5(c) summarize the results presented in Fig. 4 confirming that thinner tapers support the generation of shorter pulses. In addition, in the inset of Fig. 5(c), we compare the spectral bandwidth of three saturable absorbers with equal waist diameters (3.0  $\mu\text{m}$ ) and varying CNT concentrations. All these results confirm a pulse shortening effect resulting from (1) thinner taper waists, (2) increasing CNT concentrations, and (3) increasing intracavity powers. The pulse shortening effect has been described for other saturable absorbers [such as semiconductor saturable absorber mirrors (SESAMs)<sup>2,25</sup>], and it is known to depend on the modulation depth and level of saturation of the absorber. In CNT-PTFEMA coated tapered fiber saturable absorbers, pulse shortening results from the attenuation of the temporal wings of the pulse by the absorber.

The pulse shortening effect is not in itself unexpected; it is, however, interesting to consider a fundamental difference in terms of the dynamics of operation between saturable absorbers based on evanescent field interaction and direct interaction. Thin-film absorbers can be considered as single point absorbers with an interaction length significantly smaller than the physical length of the pulse. On the other hand, the length of interaction in CNT-polymer coated tapered fibers is of several millimeters. This means that as the pulse propagates through the tapered fiber, it experiences a dynamic absorption that varies with varying power densities at the surface and a varying ratio of power in the evanescent field as well as decreasing pulse energy.

## CONCLUSION

In this paper, we demonstrate the fabrication of low-loss carbon nanotube saturable absorbers where we exploit the evanescent field interaction of tapered fibers with a surrounding media consisting of CNTs dispersed in a low index polymer (PTFEMA). Low linear losses were achieved by improving

the method of mixing the CNTs in the polymer matrix and depositing the mixture in the tapered fibers.

A crucial benefit of reducing the losses is that it opens up the possibility of using significantly thinner and longer taper fibers, allowing us to significantly reduce the saturation power of the device. For example, in this paper, we have shown a CNT-coated taper saturable absorber with a waist diameter as thin as  $3\text{ }\mu\text{m}$  and linear losses of only 25%. This saturable absorber presents a saturation power (0.45 mW) 10 times lower than an identical device with a waist diameter of  $5.3\text{ }\mu\text{m}$  (5 mW).

The trade-off between non-saturable losses and saturation power must be considered in the fabrication of tapered fibers embedded in a low-refractive index CNT-polymer composite. With this study, we provide a guideline for the design of taper fiber-based saturable absorbers not only for carbon nanotubes but also for all other two-dimensional materials. In addition, since our procedure allows for the fabrication of devices with longer lateral interactions, they also hold promise in the exploitation of the third order nonlinearity of CNTs<sup>11,18,20</sup> where the nonlinearity of the device can be enhanced by the long length of interaction between the propagating wave and the CNT coating.

## ACKNOWLEDGMENTS

A.M. and P.L. acknowledge support from the H2020 Marie-Sklodowska-Curie Individual Fellowship scheme. M.A. acknowledges the support from the Ministry of Higher Education, Sultanate of Oman.

- <sup>1</sup> E. P. Ippen, *Appl. Phys. B: Lasers Opt.* **58**(3), 159 (1994).
- <sup>2</sup> G. Steinmeyer, D. H. Sutter, L. Gallmann, N. Matuschek, and U. Keller, *Science* **286**(5444), 1507 (1999).
- <sup>3</sup> Z. Sun, A. Martinez, and F. Wang, *Nat. Photonics* **10**(4), 227 (2016).
- <sup>4</sup> S. Y. Set, H. Yaguchi, Y. Tanaka, M. Jablonski, Y. Sakakibara, A. Rozhin, M. Tokumoto, H. Kataura, Y. Achiba, and K. Kikuchi, presented at the Optical Fiber Communication Conference, Atlanta, Georgia, 2003.
- <sup>5</sup> K. Kashiwagi and S. Yamashita, *Opt. Express* **17**(20), 18364 (2009).
- <sup>6</sup> S. Giordani, S. D. Bergin, V. Nicolosi, S. Lebedkin, M. M. Kappes, W. J. Blau, and J. N. Coleman, *J. Phys. Chem. B* **110**(32), 15708 (2006).
- <sup>7</sup> Z. Sun, T. Hasan, F. Torrisi, D. Popa, G. Privitera, F. Wang, F. Bonaccorso, D. Basko, and A. C. Ferrari, *ACS Nano* **4**(2), 803 (2010).
- <sup>8</sup> Q. Bao, H. Zhang, Y. Wang, Z. Ni, Y. Yan, Z. Shen, K. P. Loh, and D. Y. Tang, *Adv. Funct. Mater.* **19**(19), 3077 (2009).
- <sup>9</sup> R. Woodward and E. Kelleher, *Appl. Sci.* **5**(4), 1440 (2015).
- <sup>10</sup> C. Zhao, H. Zhang, X. Qi, Y. Chen, Z. Wang, S. Wen, and D. Tang, *Appl. Phys. Lett.* **101**(21), 211106 (2012).
- <sup>11</sup> J. Sotor, G. Sobon, W. Macherzynski, P. Paletko, and K. M. Abramski, *Appl. Phys. Lett.* **107**(5), 051108 (2015).
- <sup>12</sup> Y. Chen, G. Jiang, S. Chen, Z. Guo, X. Yu, C. Zhao, H. Zhang, Q. Bao, S. Wen, D. Tang, and D. Fan, *Opt. Express* **23**(10), 12823 (2015).
- <sup>13</sup> Y. Song, K. Morimune, S. Y. Set, and S. Yamashita, *Appl. Phys. Lett.* **90**(2), 021101 (2007).
- <sup>14</sup> Y. Song, S. Yamashita, C. S. Goh, and S. Y. Set, *Opt. Lett.* **32**(2), 148 (2007).
- <sup>15</sup> A. Martinez, K. Zhou, I. Bennion, and S. Yamashita, *Opt. Express* **16**(20), 15425 (2008).
- <sup>16</sup> S. Y. Choi, F. Rotermund, H. Jung, K. Oh, and D. Yeom, *Opt. Express* **17**(24), 21788 (2009).
- <sup>17</sup> K. Kieu and M. Mansuripur, *Opt. Lett.* **32**(15), 2242 (2007).
- <sup>18</sup> B. Xu, M. Omura, M. Takiguchi, A. Martinez, T. Ishigure, S. Yamashita, and T. Kuga, *Opt. Express* **21**(3), 3651 (2013).
- <sup>19</sup> S. Yamashita, *J. Lightwave Technol.* **30**(4), 427 (2012).
- <sup>20</sup> M. Sumetsky, Y. Dulashko, and A. Hale, *Opt. Express* **12**(15), 3521 (2004).
- <sup>21</sup> K. F. Lee, Y. Tian, H. Yang, K. Mustonen, A. Martinez, Q. Dai, E. I. Kauppinen, J. Malowicki, P. Kumar, and Z. Sun, *Adv. Mater.* **29**(24), 1605978 (2017).
- <sup>22</sup> W. Li, B. Chen, C. Meng, W. Fang, Y. Xiao, X. Li, Z. Hu, Y. Xu, L. Tong, H. Wang, W. Liu, J. Bao, and Y. Ron Shen, *Nano Lett.* **14**(2), 955 (2014).
- <sup>23</sup> H. A. Haus, *J. Appl. Phys.* **46**(7), 3049 (1975).
- <sup>24</sup> X. M. Liu, H. R. Yang, Y. D. Cui, G. W. Chen, Y. Yang, X. Q. Wu, X. K. Yao, D. D. Han, X. X. Han, C. Zeng, J. Guo, W. L. Li, G. Cheng, and L. M. Tong, *Sci. Rep.* **6**, 26024 (2016).
- <sup>25</sup> R. Paschotta and U. Keller, *Appl. Phys. B: Lasers Opt.* **73**(7), 653 (2001).